trochemical potential for different cystalline structures of RuO_2 films. At high temperatures, when the crystalline phase was formed, the proton only reacts with the Ru ion on the surface of the RuO_2 film. For the amorphous phase of RuO_2 films prepared at low temperatures, the proton can diffuse into the bulk of the RuO_2 film. This result is consistent with that obtained from the $RuO_2 \cdot xH_2O$ powders prepared by aqueous sol-gel technique.

Acknowledgment

The authors thank Dr. Deryn Chu for use of the low noise cyclic voltammetric system.

Manuscript received Aug. 18, 1995.

Army Research Laboratory assisted in meeting the publication costs of this article.

REFERENCES

1. S. Trasatti and G. Lodi, in *Electrodes of Conductive Metallic Oxides, Part A*, p. 301, S. Trasatti, Editor, Elsevier, New York (1980).
2. S. Ardizzone, G. Fregonara, and S. Trasatti, *Electrochim. Acta*, **35**, 263 (1990).
3. D. Michell, D. A. J. Rand, and R. Woods, *J. Electroanal. Chem.*, **89**, 11 (1978).
4. I. D. Raistrick, in *The Electrochemistry of Semiconductors and Electronics Processes and Devices*, p. 297, J. McHardy and F. Luduig, Editors, Noyes, Park Ridge, NJ (1992).
5. J. P. Zheng and T. R. Jow, *This Journal*, **142**, L6 (1995).
6. J. P. Zheng, P. J. Cygan, and T. R. Jow, *ibid.*, **142**, 2699 (1995).
7. Q. X. Jia, X. D. Wu, S. R. Foltyn, A. T. Findikoglu, P. Tiwari, J. P. Zheng, and T. R. Jow, Submitted.
8. B. E. Conway, in *Proceeding of the Second International Seminar on Double Layer Capacitors and Similar Energy Storage Devices*, Deerfield Beach, FL, Dec. 7-9, 1992.
9. A. Kozawa, Abstract 29, p. 75, The Electrochemical Society Extended Abstracts, Vol. 73-2, Boston, MA, Oct. 7-11, 1973.
10. K. Zaghib, K. Tatsumi, H. Abe, T. Ohsaki, Y. Sawada, and S. Higuichi, in *Rechargeable Lithium and Lithium-Ion Batteries*, S. Megahed, B. M. Barnett, and L. Xie, Editors, PV 94-28, p. 121, The Electrochemical Society Proceedings Series, Pennington, NJ (1995).
11. T. R. Jow and C. C. Liang, *This Journal*, **129**, 1429 (1982).
12. J. P. Zheng, D. H. Kim, S. Y. Dong, C. Lahane, W. P. Shen, and H. S. Kwok, *AIP Conference Proceedings*, Vol. 273, p. 437 (1992).
13. T. R. Jow and J. P. Zheng, *Proc. Mater. Res. Soc. Symp.*, **393** (1995).

Microcontact Printing of Alkanethiols on Silver and Its Application in Microfabrication

Younan Xia,* Enoch Kim, and George M. Whitesides

Department of Chemistry, Harvard University, Cambridge, Massachusetts 02138, USA

ABSTRACT

This paper describes the use of microcontact printing (μCP) to generate patterned self-assembled monolayers (SAMs) of alkanethiolates on the surfaces of evaporated films of silver. Using patterned SAMs of alkanethiolates as nanometer-thick resists, patterned microfeatures of silver with sizes down to ~200 nm were fabricated on Si/SiO_2 by selective etching in aqueous solutions containing $K_2S_2O_3$, $K_3Fe(CN)_6$, and $K_4Fe(CN)_6$. Complete etching of silver can be achieved more rapidly than that of gold: ~20 s *vs.* ~20 min for 50 nm thick metal films when similar ferricyanide etchants were used. Microstructures of silver produced by the present method have higher edge resolution (typically, ~20 nm *vs.* ~100 nm) and far fewer defects (~10 pits/mm^2 *vs.* ~10^3 pits/mm^2) than those of gold fabricated by a similar procedure. Silver lines (0.2 μm in thickness, ~50 μm in width, and ~5 mm in length) had the expected metallic conductivity (≈5.56 × 10^5 S/cm). parallel lines of silver (0.2 μm in thickness, ~10 μm in width, ~1 mm in length, and separated by ~10 μm) were electrically isolated from each other. Aqueous solutions containing other coordinating ligands and oxidants, $Fe(NO_3)_3$, NH_4OH/O_2, NH_4OH/H_2O_2, and H_2NCH_2COOH/H_2O_2, were also selective etchants for use with patterned SAMs of alkanethiolates on silver. Patterned structures of silver (50 nm thick) on Si/SiO_2 could be used as secondary masks for etching of SiO_2 in aqueous solutions of HF/NH_4F, and of Si(100) in aqueous solutions of KOH and *i*-propanol. Patterned films of silver (0.2 μm thick) on silicon wafers could be used as masters to cast elastomeric stamps with surface relief to be used for μCP. By choosing appropriate etching conditions, microparticles of MX (M = Ag; X = Cl, Br, I, OH, and SCN) could be formed *in situ* on the underivatized regions of the SAM-patterned surface during etching of silver.

Introduction

Microcontact printing (μCP)[1] is a convenient technique for generating patterned self-assembled monolayers (SAMs)[2] of alkanethiolates on gold,[1] and of alkylsiloxanes on silicon dioxide.[3] In carrying out μCP on gold, an elastomeric stamp is fabricated by casting polydimethylsiloxane (PDMS) against a master (usually prepared using photolithography or micromachining,[4,5] or from an available relief structure such as a diffraction grating) that provides a pattern complementary to that to be reproduced. The stamp is "inked" with a solution of alkanethiol in ethanol, the solvent evaporated, and the stamp brought into contact with the surface of the gold for 5 to 10 s. Patterned SAMs of alkanethiolates with dimensions larger than 500 nm can be produced routinely using this technique; smaller features (~100 nm) have also been generated, albeit less reproducibly.[5-7] This procedure relies for its success on the rapid reaction of alkanethiols on gold with formation of SAMs, and on the autophobicity of the resulting SAMs.[8] Patterned SAMs of hexadecanethiolate on gold serve as nanometer-thick resists that protect the underlying gold

* Electrochemical Society Student Member.

from certain etchants (for example, an aqueous solution containing CN^-/O_2 or $S_2O_3^{2-}/Fe(CN)_6^{3-}/Fe(CN)_6^{4-}$).[9-11] This combination of μCP and selective etching has been used to produce patterned features of gold on Si/SiO_2.[10,12]

Alkanethiols also form ordered SAMs on the surfaces of silver.[13] Silver has a number of advantages over gold. First, it is less expensive. Second, silver has the highest thermal conductivity and the lowest electrical resistivity among all metals: 4.29 W cm^{-1} K^{-1} and 1.59 μΩ cm.[14,15] Third, silver and silver oxide have a range of redox activities that make them useful in catalysis and electrochemical energy storage.[16] Fourth, wet etching protocols for silver are easier than those for gold because silver is chemically more reactive. Fifth, silver can be oxidized easily to form insulating layer of oxide on the surface; this property is useful for fabricating metal/insulator/metal tunneling junctions.[16,17] Sixth, as we discuss in the next section, microstructures of silver that are produced by the combination of μCP of hexadecanethiol and selective etching in solutions containing $S_2O_3^{2-}$ and $Fe(CN)_6^{3-}/Fe(CN)_6^{4-}$ have higher edge resolution and far fewer defects than those of gold fabricated using a similar procedure.

Here we demonstrate that μCP can be used to form patterned SAMs of alkanethiolates on the surfaces of evaporated silver films, and that these patterned SAMs are effective resists that protect the derivatized regions of silver from etching in a variety of aqueous etchants, for example, $Fe(NO_3)_3$, $K_2S_2O_3/K_3Fe(CN)_6/K_4Fe(CN)_6$, KCN/O_2, CH_3OH/O_2, NH_4OH/H_2O_2, and H_2NCH_2COOH/H_2O_2.

Experimental

Materials and substrates.—Ag (99.9999%), Au (99.999%), Ti (99.99%), $K_2S_2O_3$, KSCN, $K_3Fe(CN)_6$, $K_4Fe(CN)_6$, $Fe(NO_3)_3$, HF (48%, w/w), and $CH_3(CH_2)_{15}SH$ were obtained from Aldrich. KI, KBr, KCl, KOH, KCN, and NH_4OH (w/w, 28%) were purchased from Fisher Scientific. PDMS elastomer (Sylgard 184) was obtained from Dow Corning. Si(100) wafers (Cz, N/Phos.-doped, test grade, SEMI Std. flats., covered by native or thermal oxide) were obtained from Silicon Sense, Inc. (Nashua, NH). Hexadecanethiol was purified under nitrogen by chromatography through silica gel. Thin films of silver (50 to 1500 nm thick) and gold (50 nm thick) were prepared by E-beam evaporation onto silicon wafers that had been primed with titanium (2- to 3 nm thick). After evaporation, the substrates covered

Table I. Solutions that have been examined for use with patterned SAMs on silver.

Oxidant[a]	Coordinating ligand[a]	Etching rate[b]	Selectivity[c]
$K_3Fe(CN)_6$ (0.01)	None	−	—
	$K_2S_2O_3$ (0.1)	++	++
	NH_4OH (8.2)	++	+
	NH_4OH (0.16)	+	+
	KSCN (0.1)	+	+
	KCl (0.1)	+	+
	KBr (0.1)	+	+
	KI (0.1)	+	+
$Fe(NO_3)_3$ (0.05)	None	++	++
O_2 (saturated)	KCN (0.01)	+	++
	NH_4OH (8.2)	+	+
	H_2NCH_2COOH (0.1)	−	—
	KSCN (0.01)	−	—
	$K_2S_2O_3$ (0.01)	−	—
H_2O_2 (0.17)	NH_4OH (0.16)	+	+
	H_2NCH_2COOH (0.1)	+	+
$FeCl_3$ (0.01)	KCl (0.1)	0	−
	KI (0.1)	+	−
I_2 (0.005)	KI (0.1)	++	−

[a] (Concentration, *M*).
[b] All etchings were carried out at room temperature.
++ = very rapid (10 to 30 Å/s).
+ = rapid (1 to 10 Å/s).
0 = slow (< 1 Å/s).
− = very slow (almost no etching).
[c] Key: ++ = excellent, + = good, 0 = fair, − = poor, — = not examined because the etching was too slow. The evaluation of selectivity was based on the density of defects (using SEM) produced in the SAM-covered regions after the underivatized regions of silver just completely (or close to) dissolved.

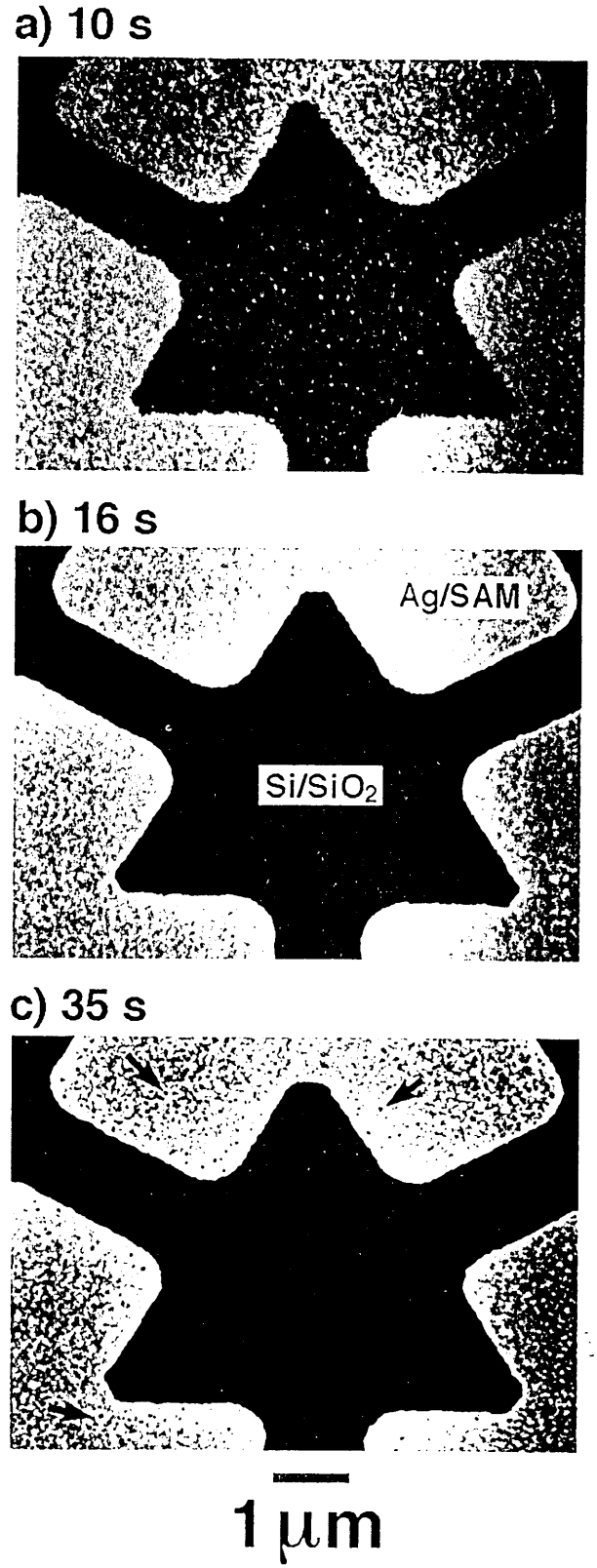

Fig. 1. SEM images of silver films (50 nm thick) that had been patterned with SAMs of hexadecanethiolate using μCP, and etched in the standard ferricyanide etchant for different intervals of time. The etching rate in this etchant was estimated to be 3 to 4 nm/s. Defects appeared in the SAM-covered regions when the samples were overetched. Three representative defects (black dots) are indicated by arrows in (c).

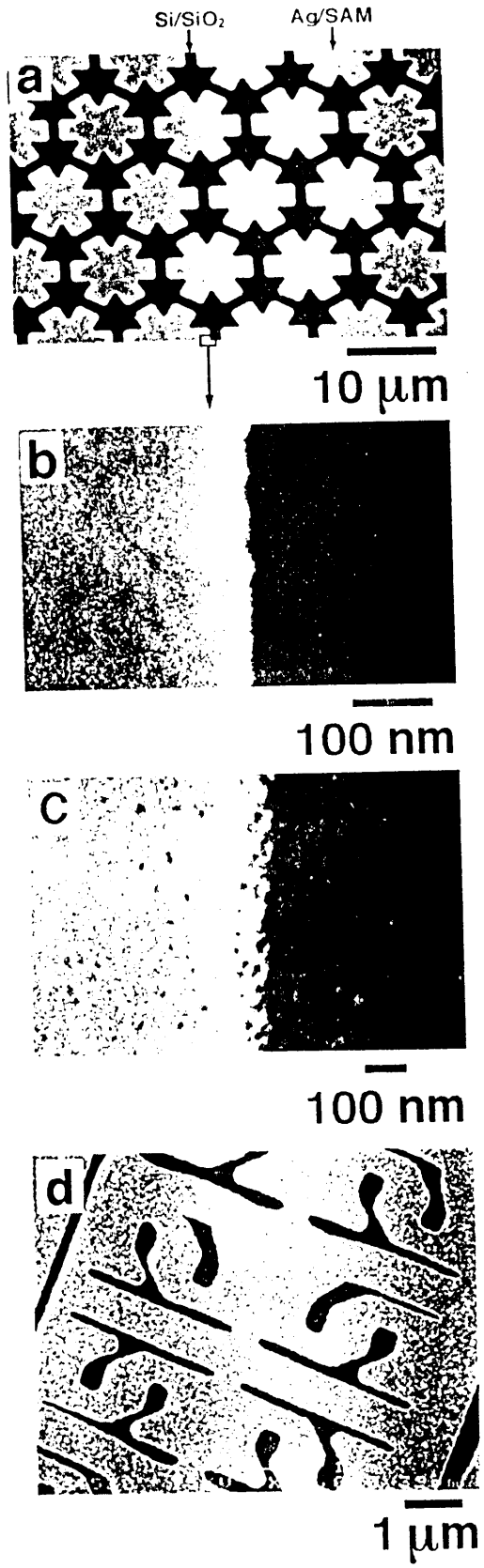

Fig. 2. (a, b) SEM images of a test pattern of silver (50 nm thick) that was fabricated by μCP with hexadecanethiol, followed by etching in the standard ferricyanide etchant for ~20 s. (c) SEM of a test pattern of gold (50 nm thick) that was fabricated by μCP, followed by selective etching in the ferricyanide etchant for ~16 min. (d) The smallest features (~200 nm in size) that have been produced in silver films (40 nm thick) by the standard combination of μCP and selective wet etching (~15 s). The bright regions are metals covered by SAMs, the dark regions are Si/SiO$_2$ where underivatized metals have dissolved.

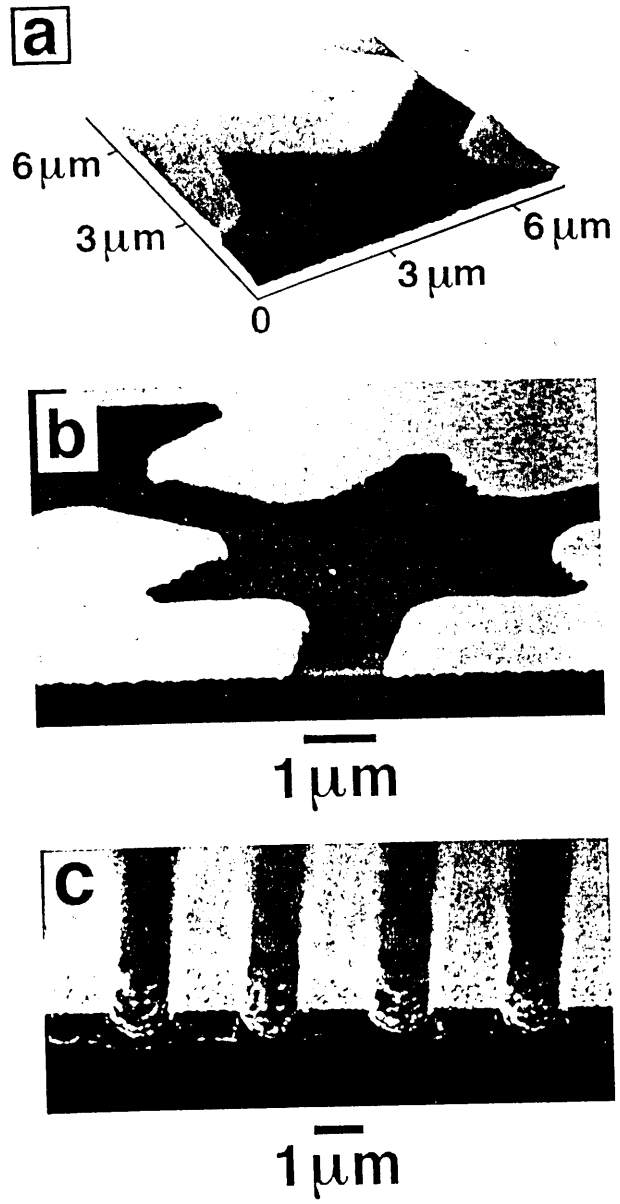

Fig. 3. (a) An AFM image of a test pattern of silver (50 nm thick) that was produced by μCP and selective etching (~20 s). (b, c) Cross-sectional SEM images of test patterns that were generated in silver films (0.2 μm and 1 μm thick) using the standard combination of μCP with hexadecanethiol and selective etching (~45 and ~90 s, respectively). The isotropic nature of the etching is clearly seen in (c).

by thin films of silver were kept in air and were used within several days. These films of silver were probably covered by an ultrathin layer of silver oxide, although x-ray photoelectron spectroscopy (XPS) of these silver surfaces only showed characteristic peaks of Ag(0); the positions of these peaks were not sensitive to the presence of very small amounts of silver oxide.[17] No difference in the quality of the silver patterns was observed for those samples fabricated from substrates that had been kept in the laboratory for different periods of time up to one month.

In this paper, 50 nm thick films of silver were used as the "standard films" in examining and comparing the etching behaviors of different etchants. There was no particular reason for choosing this thickness. Silver films as thin as 30 nm and as thick as 1 μm were also used in testing ferricyanide etchant: films 30 nm thick behaved essentially the same as those 50 nm thick; films thicker than 0.2 μm resulted in more defects in the SAM-covered regions and

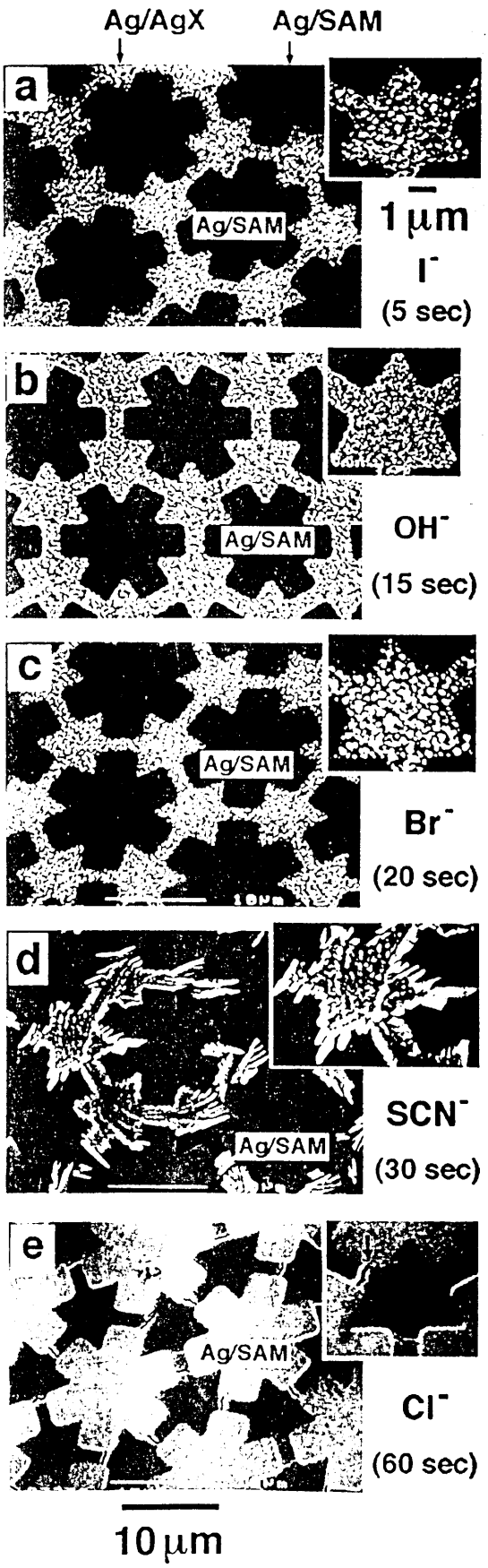

Fig. 4. SEM images of test patterns of silver (50 nm thick) that were produced by etching in the ferri/ferrocyanide solutions, with KI, NH_4OH, KBr, KSCN, and KCl as the coordinating ligands. Due to their low solubilities in water, AgX precipitated *in situ* on the underivatized regions of the SAM-patterned surfaces of silver. The cracks formed in AgCl (indicated by arrows in e) probably resulted from drying the sample too rapidly.

lower edge resolution for the generated microstructures of silver than films 50 nm thick. We believe that for each etchant there is a thickness that optimizes cost and edge resolution; and minimizes the density of defects.

Microcontact printing (μCP).—PDMS stamps were fabricated according to the published procedure.[1,10] Before printing, silver substrates were rinsed with ethanol and dried in a stream of N_2. An ~2 m*M* solution of hexadecanethiol in ethanol was used as the "ink." After applying the hexadecanethiol solution (with cotton Q-tip) to the PDMS stamp, the stamp was dried in a stream of N_2 for ~1 min, and brought into contact with the surface of silver for 5 to 10 s.

Etching of silver and gold.—The composition of the standard ferri/ferrocyanide etchant for silver was: $K_2S_2O_3$ (0.1 *M*), $K_3Fe(CN)_6$ (0.01 *M*), and $K_4Fe(CN)_6$ (0.001 *M*). **Caution**: *Potassium ferricyanide is light sensitive. The photodecomposed products contain free cyanide. Potassium ferricyanide is also incompatible with acids and releases HCN.* All etchings of silver were conducted using this solution unless otherwise mentioned. For those ferri/ferrocyanide etchants using I^-, Br^-, Cl^-, and SCN^- as the coordinating ligands, $K_2S_2O_3$ was substituted by the same concentration of KI, KBr, KCl, or KSCN. The composition of the cyanide etching solution for silver was: KOH (1 *M*) and KCN (0.1 *M*). The ferri/ferrocyanide etching solution for gold was: [11]$K_2S_2O_3$ (0.1 *M*), $K_3Fe(CN)_6$ (0.01 *M*), $K_4Fe(CN)_6$ (0.001 *M*), and KOH (1 *M*). All etching of silver was carried out at room temperature in a 400 ml beaker with ~300 ml etchant. The etching solution was stirred at ~300 rpm with a magnetic stirring bar that was ~2 cm long. The etching time reported here represents the minimum time (or close to the minimum time) that is required to dissolve completely the underivatized silver film having the indicated thickness in the indicated etchant. This time was obtained by examining [using scanning electron microscopy (SEM)] silver samples that have been patterned with hexadecanethiol by μCP, and etched for different intervals of time (for example, as shown in Fig. 1).[11]

Etching of silicon.—Anisotropic etching of silicon was carried in an aqueous solution containing KOH and *i*-propanol (*i*-PrOH) at 65°C (400 ml of H_2O, 92 g of KOH, 132 ml of *i*-PrOH) for ~10 min.[12] The etching solution was stirred at ~300 rpm. Before etching the silicon, the native oxide on the silicon was removed by dipping the samples in an aqueous solution of HF/NH_4F (250 ml of H_2O, 140 ml of 48% HF, and 65.5 g of NH_4F) for ~1 min.

Instrumentation.—SEM was done on a JEOL JSM-6400 scanning electron microscope. Atomic force microscopy (AFM) image was obtained using a Topometrix TMX 2010 scanning electron probe microscope (Mountain View, CA); the images were obtained in the contact mode.

Results and Discussion

A chemical etchant must contain an oxidant and a coordinating ligand in order to dissolve a metal.[11] For silver, the oxidant can be Fe(III), O_2, or H_2O_2; the coordinating ligand can be $S_2O_3^{2-}$, CN−, X− (X=I, Br, Cl, OH, and SCN), NH_3, amino acids, or NO_3^-.[18-22] Table I surveys some aqueous solutions that have been examined as etchants for use with patterned SAMs of alkanethiolates on silver. Most of them are effective etchants for silver, and many have good to excellent selectivity.

Etching solutions that use $K_3Fe(CN)_6$ as the oxidant.—Figure 1 shows scanning electron micrographs (SEMs) of silver films (50 nm thick) that had been patterned with SAMs of hexadecanethiolate using μCP and etched in the standard ferricyanide etchant for different intervals of time. In the SEMs, the bright regions are silver covered by the SAM and the dark regions are Si/SiO_2 where the underivatized silver has dissolved. The progression of dissolution of bare silver can be clearly seen from these SEM images. Since silver is chemically more reactive than gold, no KOH is required in the etching solution to achieve

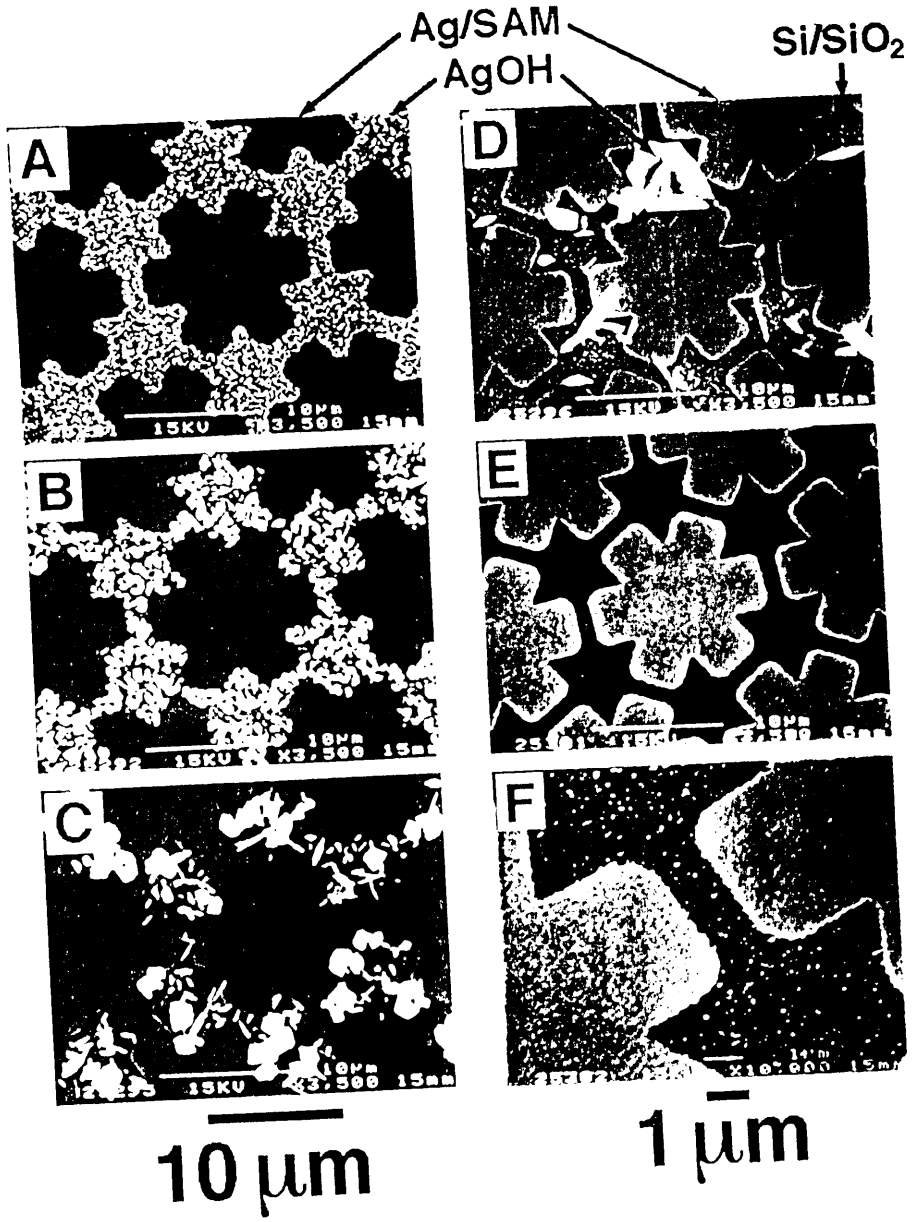

Fig. 5. SEM images of test patterns of silver (50 nm thick) that were generated by μCP with hexadecanethiol, followed by etching for ~15 s in the ferri/ferrocyanide solutions (0.01/0.001 *M*) with different concentrations of NH_4OH. (A) 0.5, (B) 1.0, (C) 1.5, (D) 2.0, and (E,F) 3.0 *M*. No AgOH precipitate was produced due to the formation of complexes of silver at high concentrations (≥2 *M*) of NH_4OH. The 10 μm bar applies to Fig. A-E. The edge resolution in this etchant is ~200 nm. The light specks on the dark regions (E, F) are remaining islands of silver.

rapid and selective etching.[11] The time required for the complete dissolution of 50 nm thick silver films in this standard ferricyanide etchant was ~16 s; the etching window was ~10 s.[11] During the first ~26 s, silver dissolved only from the bare regions; when samples were etched for longer periods of time, defects appeared in the SAM-covered regions (Fig. 1c). Reducing the concentration of $S_2O_3^{2-}$ from 0.1 to 0.01 *M* decreased the etching rate by ~30%, but had no influence on the etching window.[11]

Figures 2a and b show SEM images (at two different magnifications) of a test pattern of silver (50 nm thick) fabricated by etching in the standard ferricyanide etchant for ~20 s, with a patterned SAM of hexadecanthiolate as the resist. Figure 2c shows the SEM of a test pattern of gold (50 nm thick) that was fabricated using a similar procedure.[11] The microstructures of silver fabricated by μCP and selective wet etching have higher edge resolution (~20 *vs.* ~100 nm) and far fewer defects (~10 pits/mm^2 *vs.* ~10^3 pits/mm^2) than those of gold produced by a similar procedure.[23] The SAM of hexadecanethiolate formed by μCP has an edge resolution of < 50 nm as characterized by AFM studies.[24] The edge resolution of the silver structures (50 nm thick) therefore probably represents the low limit for microstructures that can be fabricated by μCP and selective wet etching using current techniques. Different etchants usually result in different edge resolutions, as can be seen from the results of next several sections. The difference in the density of defects (using similar etchants) between the microstructures of silver and gold may be due to the structural differences between the SAMs of hexadecanethiolate on silver and gold: the alkanethiolates on silver have a smaller tilt angle (~12° *vs.* ~30°), and as a result, fewer domains than those on gold.[2,25] At present, the smallest features produced by the standard procedure of μCP and selective etching are ~200 nm in size (Fig. 2d). These dimensions are set by the stamps that were available for use with this work; we have not tried stamps with smaller features, and the lower limit to the definition that can be achieved by this technique is not established by the present work.

Figure 3 gives detailed profiles of the edges of the microstructures etched in silver films. Figure 3a is an AFM

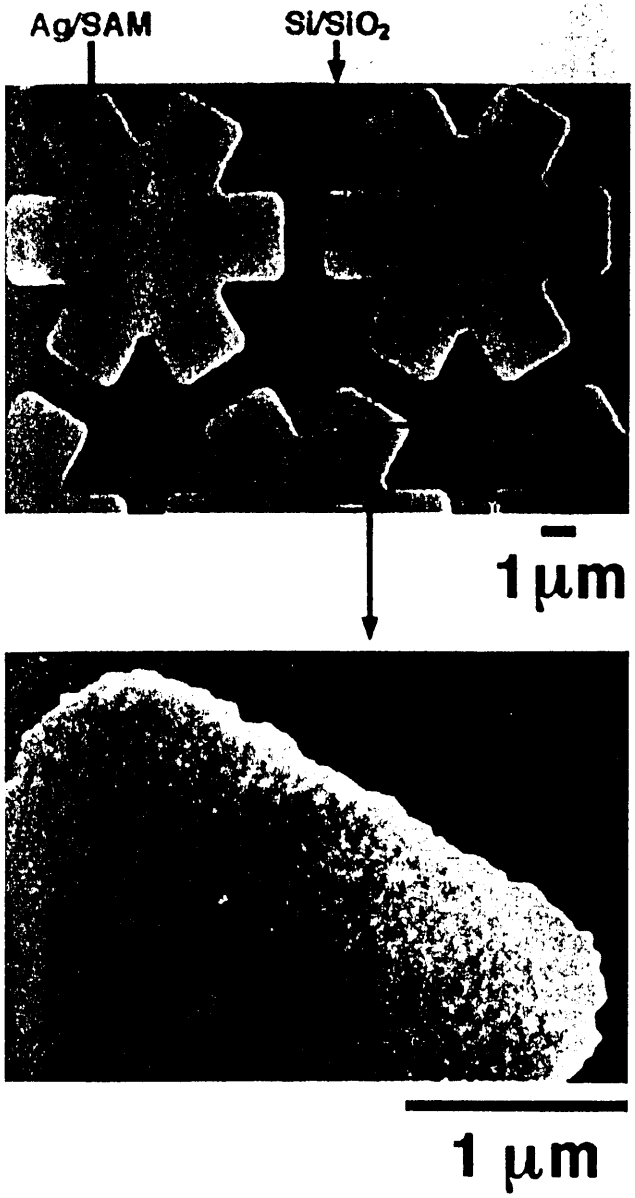

Fig. 6. SEM image of a silver pattern (50 nm thick) that was generated by etching in aqueous $Fe(NO_3)_3$ solution (0.05 *M*) for ~30 s, with printed SAMs of hexadecanethiolate as the resists.

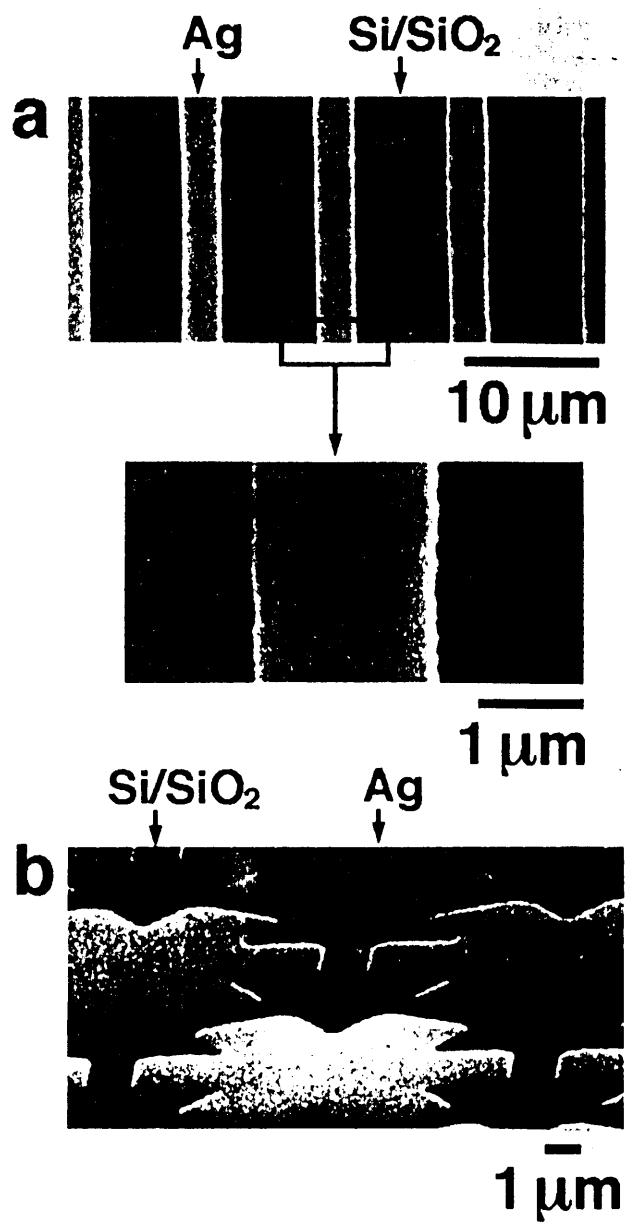

Fig. 7. SEMs of a test pattern of silver (50 nm) that was generated using μCP with hexadecanethiol, followed by etching in solutions saturated with oxygen, for ~2 min with KCN (0.1 *M*) as the coordinating ligand (a), and for ~9 min with NH_4OH (8.2 *M*) as the coordinating ligand (b).

image of a test pattern of silver fabricated in a 50 nm thick film, and Fig. 3b is a cross-sectional SEM image of the same test pattern fabricated in a 200 nm thick film. Both patterns of silver were generated using μCP with hexadecanethiol, followed by etching in the standard ferricyanide solution for ~20 and ~45 s, respectively. The etching of silver in the standard ferricyanide etchant was isotropic (Fig. 3d).

Figure 4 shows SEM images of silver samples (50 nm thick) that had been patterned with SAMs of hexadecanethiolate by μCP and etched in aqueous solutions that use ferri/ferrocyanide (0.01/0.001 *M*) as the oxidant, and KI (0.1 *M*), KCl (0.1 *M*), KBr (0.1 *M*), KSCN (0.1 *M*), and NH_4OH (0.16 *M*) as the coordinating ligand, respectively. The AgX microcrystals (<0.5 μm in size) on the underivatized regions were formed by the reaction indicated in Eq. 1

$$Ag(s) + Fe(CN)_6^{3-}(aq) + X^-(aq) = AgX(s) + Fe(CN)_6^{4-}(aq)$$

$$X = I, Br, Cl, OH, \text{and } SCN) \quad [1]$$

The composition of MX (M = Ag; X = I, Br, Cl, OH, and SCN) was verified qualitatively by energy dispersed spectroscopy (EDS). The rate of etching decreased in the order of $I^- > OH^- \approx Br^- \approx SCN^- > Cl^-$; an order that was probably determined by the solubility-product constants (K_{sp}) of the resulting precipitates. The silver seemed to dissolve into solution first, and then AgX crystals grew from the solution onto the surfaces. These AgX precipitates could not be dissolved by water; all of them could be easily dissolved by immersing the samples in an aqueous solution containing $K_2S_2O_3$ (~0.1 *M*) for ~30 s

$$AgX(s) + 2S_2O_3^{2-}(aq) = Ag(S_2O_3^{2-})_2^{3-}(aq) + X^-(aq)$$

$$(X = I, Br, Cl, OH, \text{and } SCN) \quad [2]$$

Silver films (~50 nm thick) underivatized by SAMs did not completely dissolve in these five etching solutions because the AgX precipitate formed a barrier between the silver surface and the etchant during etching. Nevertheless,

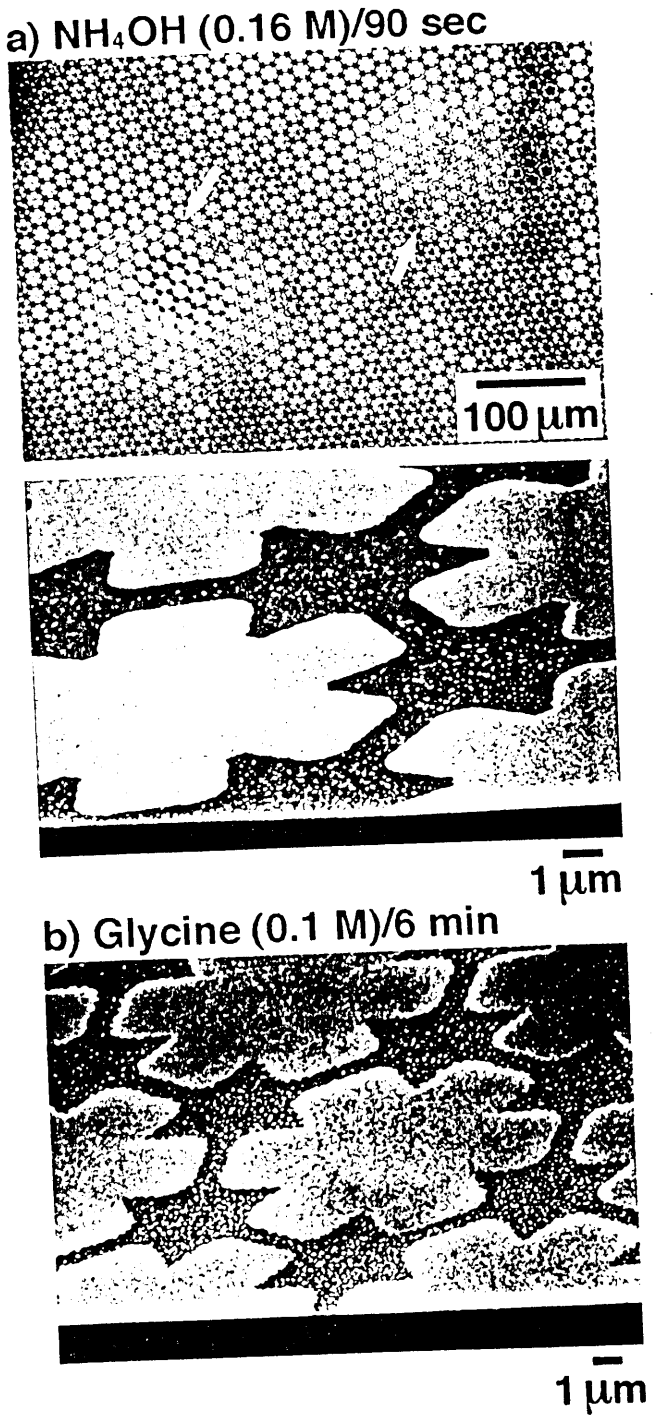

Fig. 8. SEM images of silver patterns (50 nm thick) that were produced by etching in solutions that used H_2O_2 (0.17 *M*) as the oxidant and (a) NH_4OH (0.16 *M*), (b) H_2NCH_2COOH (0.1 *M*) as the coordinating ligand. Oxygen bubbles formed from the decomposition of H_2O_2 (indicated by arrows in (a) blocked the the access of etchants to the surface and slowed the etching on those areas covered by bubbles. Note that the edges of the silver patterns are extremely rough (300 nm) in this etchant. The blemishes on the etched regions were remaining islands of silver.

this result provides a new approach for forming patterned microcrystals of AgX on the surface, and (at least for Cl^-) for contouring the surface.

The precipitate of AgOH is soluble in highly concentrated solutions (>2 *M*) of NH_4OH.[26] Figure 5 shows SEMs of silver samples (50 nm thick) that were patterned with a SAM of hexadecanethiolate and that had been etched for ~15 s in ferri/ferrocyanide (0.01/~0.001 *M*) solutions with different concentrations of NH_4OH. Since the concentration of AgOH was determined by the concentration of NH_4OH, here we observed a transition from homogeneous to heterogeneous nucleation when the concentration of NH_4OH changed from 0.5 to 2.0 *M*. At higher concentrations of NH_4OH, either no AgOH crystals were formed, or this material dissolved immediately after formation

$$AgOH(s) + 2NH_4OH(aq) = Ag(NH_3)_2^+(aq) + OH^-(aq) + 2H_2O \quad [3]$$

Etching solutions that use $Fe(NO_3)_3$ as the oxidant.—$AgNO_3$ is soluble in water at room temperature. Thus, $Fe(NO_3)_3$ could be used as a selective etchant for silver in a single-component solution

$$Ag(s) + Fe(NO_3)_3(aq) = AgNO_3(aq) + Fe(NO_3)_2(aq) \quad [4]$$

Figure 6 shows SEM images of a test pattern of silver (50 nm thick) that was generated by etching in an aqueous solution of $Fe(NO_3)_3$ (0.05 *M*) for ~30 s. The edge resolution of the silver structures that were fabricated using this etchant is ~100 nm. The etching rate increased linearly as the concentration of $Fe(NO_3)_3$ increased from 0.01 to 0.1 *M* Eq. 5

$$\text{Etching rate (nm/s)} \approx 46.7\ [Fe(NO_3)_3]\ (M) \quad [5]$$

Although the edge resolution of this etchant is not as good as that of ferri/ferrocyanide, the low toxicity and cost of $Fe(NO_3)_3$ makes this etchant attractive in many applications.

Etching solutions that use O_2 as the oxidant.—Figure 7a shows SEM images of silver lines (50 nm thick) fabricated by µCP of hexadecanethiol, followed by etching for ~2 min in an aqueous KCN solution (pH ≈ 14, [KCN] ≈ 0.1 *M*) saturated with O_2. Note that complete etching of gold films with the same thickness in an etching solution with the same composition usually takes ~30 min.[11] The edge resolution of silver features fabricated using this etchant is ~100 nm. Unfortunately, the highly toxicity and environmental impact of free cyanide ion makes this etchant unattractive in many applications.

When ligands that coordinate with silver more weakly than cyanide were used, etching of silver became much slower (Table I). Figure 7b shows SEMs of silver patterns that were generated by selective etching in aqueous NH_4OH solution (8.2 *M*) for 6 min, with O_2 (from air) as the oxidant.

Etching solutions that use H_2O_2 as the oxidant.—Figure 8 shows SEM images of silver patterns that were generated by µCP with hexadecanethiol, and selective etching in solutions that used H_2O_2 as the oxidant, with NH_4OH and H_2NCH_2COOH as the coordinating ligand, respectively. During etching, oxygen from the decomposition of H_2O_2 formed small bubbles on the surfaces of the samples. As a result, the etched surfaces became heterogeneous: areas not covered by bubbles etched more rapidly than those covered by bubbles (Fig. 8a). This etchant is therefore not recommended for practical applications. There was another difference between the systems that used H_2O_2 and ferri/ferrocyanide as the oxidants: no AgOH precipitate was formed at this low concentration of NH_4OH (0.16 *M*) for the H_2O_2 system.

Electrical conductivity and isolation of silver lines.—Using the standard combination of µCP and selective wet etching, an interdigitated array of silver lines (0.2 µm thick, ~10 µm in width, ~1 mm in length, and separated by ~10 µm) was fabricated on a silicon wafer that was covered by a 0.5 µm thick thermal SiO_2 layer. The sample was subsequently immersed in an aqueous solution of HF (w/w, ~1%) for ~0.5 min to dissolve the exposed regions of the titanium film (2 to 3 nm thick) that was used as the primer between silver and silicon.[27] The resistance across this array was measured to be ~2 MΩ. This value is about six orders of magnitude higher than that measured on con-

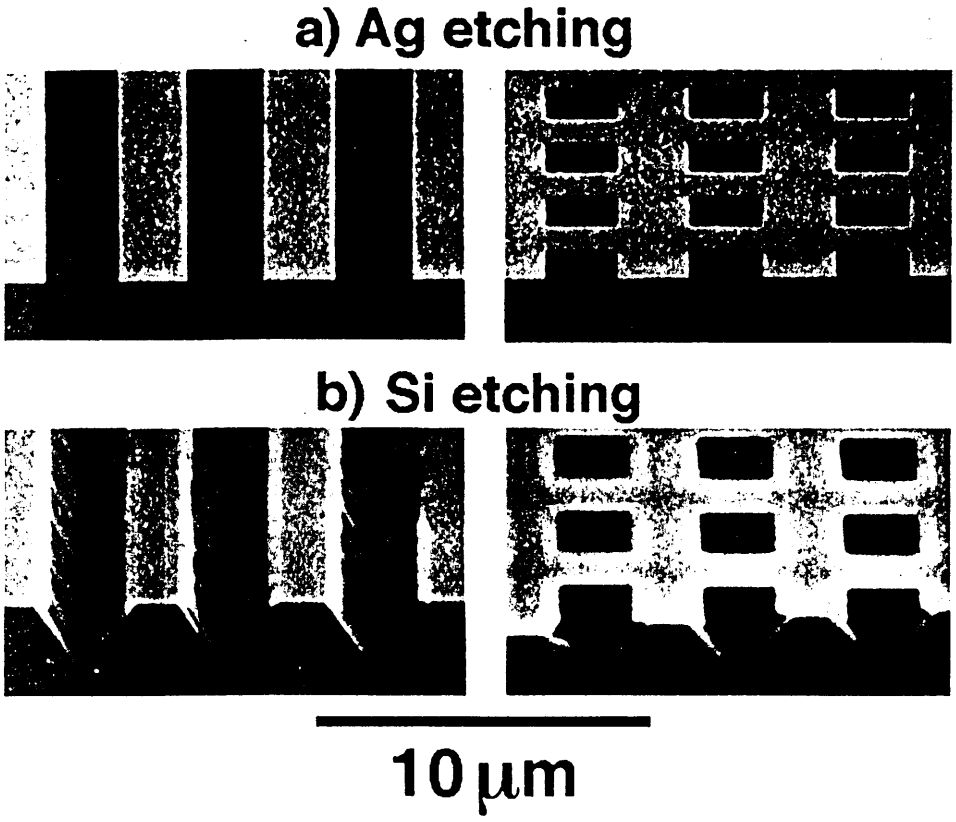

Fig. 9. (a) SEMs of silver patterns (50 nm thick) that were generated using the combination of μCP and selective wet etching. The bright regions are metals covered by SAMs, the dark regions are Si/SiO_2 where underivatized metals have dissolved. (b) SEMs of samples after anisotropic etching of silicon in KOH/*i*-PrOH at 65°C for ~10 min with the above patterned silver films as the masks. The silver masks remained on the surfaces.

tinuous regions of silver films, indicating that the silver lines that are ~10 μm in separation are electrically isolated from each other.

Silver lines (~0.2 μm thick, ~50 μm in width, and ~5 mm in length) suitable for the measurement of conductivity were also fabricated using a similar method. A resistivity of ~1.8 μΩ cm was measured using the two-probe method. This value is close to the resistivity reported for bulk silver, ~1.6 μΩ cm[15]; this value indicates that the silver lines fabricated by the present method have the expected metallic conductivity.

Patterned films of silver as masks for the etching of SiO_2 and Si.—One of the applications of μCP on coinage metals (combined with selective wet etching) is using patterned structures of these metals as secondary masks for the etching of underlying layers of SiO_2 and Si.[5,12] Figure 9a shows SEM images of lines and grids of silver that were generated by the standard procedure of μCP and selective wet etching in ferri/ferrocyanide solutions. The silver films were stable in strongly alkaline solutions (~4 *M* of KOH) at elevated temperatures. After dissolving the native oxide of silicon by immersion in aqueous HF/NH_4F for ~1 min, the (100) Si wafers were anisotropically etched in KOH/*i*-propanol for ~10 min at 65°C (Fig. 9b).

Patterned structures of silver as molds for casting PDMS stamps to be used for μCP.—Since silver is relatively inexpensive and can be etched rapidly in a variety of etching solutions, we wished to determine if it could be used as a relief structure with which to fabricate PDMS stamps (Fig. 10). We cast PDMS stamps against patterned silver structures etched in silver films of 0.2 μm in thickness. Figure 11a shows a cross-sectional SEM image of the patterned structure of silver that was used to produce relief when casting the PDMS stamp; Fig. 11b shows the SEM image of the silver pattern (50 nm thick) that was generated by μCP using this PDMS stamp (after wet etching in the standard ferri/ferrocyanide solution for ~20 s). These two silver patterns are complementary to each other. This method provides a convenient route for generating negative patterns without further access to facilities for photolithography. The edge resolution of the second silver pattern is <100 nm, a value that is good enough for many applications.

Conclusions

Patterned features of silver with dimensions of less than 0.5 μm can be generated routinely by a combination of

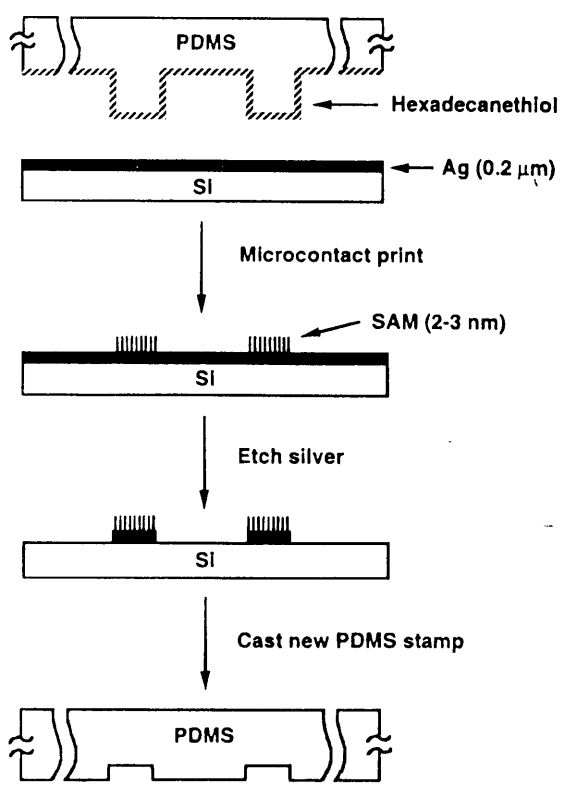

Fig. 10. A schematic outline for fabricating PDMS stamps with negative patterns from etched silver structures. Note that the thickness of the monolayer was exaggerated in the drawing.

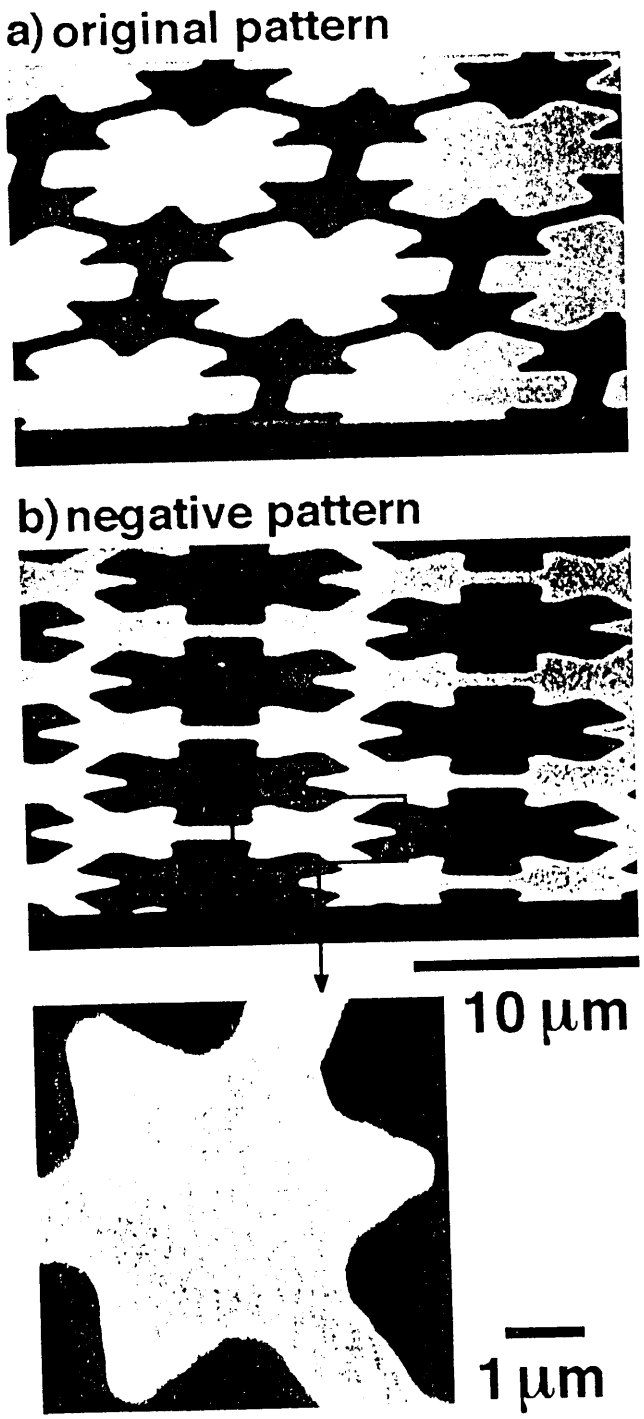

Fig. 11. (a) SEM image of the silver structure (0.2 μm thick) that was generated by μCP and selective etching (~45 s). (b, c) SEM images of the silver pattern that was produced by μCP using the PDMS stamp cast from the silver structure of (a), followed by selective etching (~45 s). The 10 μm scale bar applies to both (a) and (b). The bright regions are metals covered by SAMs, the dark regions are Si/SiO_2 where underivatized metals have dissolved.

μCP of hexadecanethiol and selective etching in a variety of aqueous solutions. Etching of silver in solutions containing $S_2O_3^{2-}$ and $Fe(CN)_6^{3-}/Fe(CN)_6^{4-}$ was much more rapid than that of gold (0.5 min *vs.* 15 min for 50 nm thick films). Typically, patterned films of silver generated using this procedure have higher edge resolution (~20 nm) and far fewer defects (~10 pits/mm^2) than those of gold (~100 nm and ~10^4 pits/mm^2). Silver lines produced on Si/SiO_2 by this method had the expected metallic conductivity and were electrically isolated using test structures. A sequence that consists of stamping a patterned SAM on silver film, removing the unprotected silver by etching, forming a new stamp from the patterned silver, restamping, and re-etching constitutes a convenient method for generating negative patterns that do not require further access to photolithography facilities. Moreover, electroplating and electroless deposition (for example, using Tollen's reagent and similar process) have been carried out at an industrial scale to make high quality coatings or mirrors (both planar and nonplanar) of silver; a combination of such plating procedures and μCP/etching may provide a convenient method for making patterned features on curved surfaces.[28] Patterning on nonplanar surfaces is difficult by current photolithographic techniques.

Acknowledgments

This work was supported in part by ONR and ARPA. This work made use of MRSEC Shared Facilities supported by the National Science Foundation (DMR-9400396). We would like to thank Yuanzhang Lu and Stephen Shepard for their assistance in using SEM and photolithographic instruments. The test pattern of Fig. 2d was kindly provided by Dr. George Maracas of Motorola Corporation. Y. X. would like to thank Joe Tien for his assistance in obtaining Fig. 3c.

Manuscript submitted July 13, 1995; revised manuscript received Oct. 7, 1995.

Harvard University assisted in meeting the publication costs of this article.

REFERENCES

1. A. Kumar and G. M. Whitesides, *Appl. Phys. Lett.*, **63**, 2002 (1993).
2. G. M. Whitesides and P. E. Laibinis, *Langmuir*, **6**, 87 (1990); L. H. Dubois and R. G. Nuzzo, *Annu. Rev. Phys. Chem.*, **43**, 437 (1992).
3. Y. Xia, M. Mrksich, E. Kim, and G. M. Whitesides, *J. Am. Chem. Soc.*, **117**, 9576 (1995).
4. Y. Xia, A. Zhuk, and G. M. Whitesides, Unpublished results.
5. J. L. Wilbur, E. Kim, Y. Xia, and G. M. Whitesides, *Adv. Mater.*, **7**, 649 (1995).
6. Y. Xia and G. M. Whitesides, *J. Am. Chem. Soc.*, **117**, 3274 (1995).
7. Y. Xia and G. M. Whitesides, *Adv. Mater.*, **7**, 471 (1995).
8. H. Biebuyck and G. M. Whitesides, *Langmuir*, **10**, 4581 (1994).
9. A. Kumar, H. Biebuyck, N. L. Abbott, and G. M. Whitesides, *J. Am. Chem. Soc.*, **114**, 9188 (1992).
10. A. Kumar, H. Biebuyck, and G. M. Whitesides, *Langmuir*, **10**, 1498 (1994).
11. Y. Xia, X.-M. Zhao, E. Kim, and G. M. Whitesides, *Chem. Mater.*, **12**, 2332 (1995).
12. E. Kim, A. Kumar, and G. M. Whitesides, *This Journal*, **142**, 628 (1995).
13. P. E. Laibinis, G. M. Whitesides, D. L. Allara, Y.-T. Tao, A. N. Parikh, and R. G. Nuzzo, *J. Am. Chem. Soc.*, **113**, 7152 (1991).
14. C. Kittel, *Introduction to Solid State Physics*, 6th ed., p. 110, John Wiley & Sons, Inc., New York (1986).
15. M. J. Hampden-Smith and T. T. Kodas, *MRS Bull.*, **6**, 39 (1993).
16. T. P. Dirske, in *Zinc-Silver Oxide Batteries*, A. Fleischer and J. J. Lander, Editors, p. 100, John Wiley & Sons, Inc., New York (1971).
17. Y. Xia, E. Kim, M. Mrksich, and G. M. Whitesides, *Chem. Mater.*, In press (1996).
18. F. A. Cotton and G. Wilkinson, *Advanced Inorganic Chemistry*, 5th ed., pp. 937-848, John Wiley & Sons, Inc., New York (1988).
19. W. Kern and C. A. Deckert, *Thin Film Processes*, J. L. Vossen and W. Kern, Editors, pp. 401-481, Academic Press, Inc., New York (1978).
20. L. J. Bousse, P. Bergveld and H. J. M. Geeraedts, *Sens. Actuat.*, **9**, 179 (1986).
21. Y. C. Guan and K. N. Han, *This Journal*, **141**, 91 (1994).

22. Y. C. Guan and K. N. Han, *ibid.*, **142**, 1819 (1995).
23. Y. Xia, X.-M. Zhao, and G. M. Whitesides, Unpublished results.
24. J. L. Wilbur, H. A. Biebuyck, J. C. MacDonald, and G. M. Whitesides, *Langmuir*, **11**, 825 (1995).
25. P. Fenter, P. Eisenberger, J. Li, N. Camillone III, S. Bernasek, G. Scoles, T. A. Ramanarayaman, and K. S. Liang, *ibid.*, **7**, 2013 (1991).
26. F. A. Cotton and G. Wilkinson, *Advanced Inorganic Chemistry*, 5th ed., p. 943, John Wiley & Sons, Inc., New York (1988).
27. W. Kern and C. A. Deckert, *Thin Film Processes*, J. L. Vossen and W. Kern, Editors, p. 471, Academic Press, Inc., New York (1978).
28. R. J. Jackman, J. L. Wilbur, and G. M. Whitesides, *Science*, **269**, 664 (1995).

Characterization of High Oxygen:Tetraethylorthosilicate Ratio Plasma-Enhanced Chemical Vapor Deposited Films

D. A. DeCrosta,* J. J. Hackenberg, and J. H. Linn

Harris Semiconductor, Melbourne, Florida 32902, USA

ABSTRACT

An investigation was conducted to characterize film properties of oxygen-rich tetraethylorthosilicate (TEOS) films deposited by single-wafer plasma-enhanced chemical vapor deposition. By increasing the oxygen:TEOS gas ratio from 1:1 to 4:1 and maintaining a reduced gas flow rate, undoped silicon glass (USG) and phosphorus-doped silicon glass (PSG) films exhibited a lower fixed charge, increased Si-O bonding sites, higher compressive film stresses, and higher refractive indexes. The USG and PSG deposition parameters were optimized to achieve a film nonuniformity of <2.7% (1σ) and deposition rates of 1500 and 3100 Å/min, respectively.

Introduction

Silicon dioxide films have been widely used in the microelectronics industry as an interlayer dielectric (ILD) film. As the size of integrated circuits continues toward submicron dimensions, the type of ILD process employed becomes more challenging due to higher aspect ratio topography and film charging considerations. Silane-based plasma-enhanced chemical vapor deposition (PECVD) films generate reasonable ILD films, but suffer from poor step coverage conformality. As interconnect pitches decrease, silane-based PECVD films suffer from incorporated voids between the interconnect lines leading to possible long-term reliability issues.[1] An alternative to silane-based films, is PECVD using TEOS as the silicon source. PECVD TEOS films exhibit good step coverage conformality, resulting in reduced film voiding between submicron features.[2] A disadvantage of TEOS PECVD films is their inherently greater film charging during deposition. Film charging affects field threshold voltage, degrading circuit performance, the magnitude of which depends on the circuit technology.[3,4] Papers have been published citing reduced film charging in TEOS PECVD films deposited in oxygen-rich gas environments.[5,6] The manufacturing feasibility and film property requirements are often not sufficiently addressed. Typical manufacturing requirements for single-wafer deposition[7] generally require a refractive index of 1.46 ± 0.01, a deposition rate of 7800 ± 300 Å/min, nonuniformity <2.5%, and a compressive film stress between 0.5 to 1.0 × 10^9 dyn/cm^2. In this paper we investigate the deposition of oxygen-rich TEOS PECVD films that can be processed meeting typical manufacturing requirements, in particular step coverage, film nonuniformity, and reduced film charging.

Experimental

Silicon wafers (150 mm, (100), n-type, 3-5 Ω-cm) were used as the substrate on which oxygen-rich (4:1 oxygen:TEOS) PECVD USG films were deposited in an Applied Materials P5000 single-wafer tool. This tool is a multichamber vacuum load lock deposition system. Experiments were designed to optimize deposition rates as a function of gas flow rate conditions. These varied from 675 to 1250 sccm, while maintaining a constant 4:1 oxygen to TEOS gas ambient. Susceptor temperature was held constant at 400°C by the use of infrared (IR) lamps. Chamber pressure during deposition was 9 Torr. The upper electrode was a showerhead design and is RF coupled to a 13.56 MHz RF power supply. Oxide deposition rates and film nonuniformity measurements were determined using a 49 point measurement with a Prometrix FT-600. Nonuniformity values were calculated using (standard deviation/mean) × 100.

The effect of susceptor spacing on film deposition was evaluated. Susceptor spacing matrices are typically performed in manufacturing to minimize nonuniformity. Oxygen-rich USG films were deposited under varying susceptor spacing ranging from 0.46 to 0.58 cm. Film deposition rates and nonuniformity values were subsequently determined.

A third experiment was conducted to determine the effects of RF power. Oxygen-rich USG phosphorous-doped silicon glass (PSG) films were deposited under varying RF power settings ranging from 300 to 550 W. Film deposition rates and nonuniformity values were obtained for each RF power setting and film type. The film stresses were measured using a Flexus 2300, and refractive index values, η, were calculated from a Rudolph ellipsometer Model Auto El.

A final experiment was designed to assess step coverage conformality, changes in Si-O bonding, film charging, and wet etch rates as RF power and gas ratios varied. USG and PSG films were deposited onto 1.2 μm thick patterned aluminum, with various pitches, to evaluate step coverage conformality. The films were deposited using an RF power of either 300 or 550 W and a gas ratio of either 1:1 (standard) or 4:1 (oxygen rich). Cross sections of the deposited films were examined using an Amray 1645 scanning electron microscope (SEM). Step coverage values were subsequently calculated. Si-O bonding and wet etch rate conditions were determined to evaluate film density as a function of power and gas ratios. USG and PSG films were deposited under the above conditions. Bonding in the films was analyzed using a Nicolet 5DBX Fourier transform infrared spectrometer (FTIR). Oxide etch rates were determined using a timed buffered oxide etch (9:1 BOE).

Measurement of film charging was achieved by depositing USG and PSG films onto wafers with 0.1 μm of ther-

* Electrochemical Society Active Member.